


RESEARCH ARTICLE

Open Access



Stalagmite evidence for East Asian winter monsoon variability and ^{18}O -depleted surface water in the Japan Sea during the last glacial period

Shota Amekawa¹, Kenji Kashiwagi², Masako Hori³, Tomomi Sone⁴, Hirokazu Kato¹, Tomoyo Okumura⁵, Tsai-Luen Yu⁶, Chuan-Chou Shen^{6,7,8} and Akihiro Kano^{1*} 

Abstract

In the East Asian monsoon area, stalagmites generally record lower and higher oxygen isotope ($\delta^{18}\text{O}$) levels during warm humid interglacial and cold dry glacial periods, respectively. Here, we report unusually low stalagmite $\delta^{18}\text{O}$ from the last glacial period (ca. 32.2–22.3 ka) in Fukugaguchi Cave, Niigata Prefecture, Japan, where a major moisture source is the East Asian winter monsoon (EAWM) that carries vapor from the warm surface of the Japan Sea. The $\delta^{18}\text{O}$ profile of this stalagmite may imply millennial-scale changes, and high $\delta^{18}\text{O}$ intervals that are related to Dansgaard–Oeschger (D–O) interstadials. More importantly, the stalagmite exhibits low overall $\delta^{18}\text{O}$ values; the mean $\delta^{18}\text{O}$ (–8.87‰) is distinctly lower than the mid-Holocene mean of another stalagmite from the same cave (4.2–8.2 ka, –7.64‰). An interpretation assuming a more intense EAWM and greater vapor transportation during the last glacial period, compared with the mid-Holocene, contradicts the limited inflow of the Tsushima Warm Current into the Japan Sea because of lowered sea level. Additionally, our model calculation using $\delta^{18}\text{O}$ data from meteoric water indicated that the amount effect of winter meteoric water was insignificant (1.2‰/1000 mm). Low stalagmite $\delta^{18}\text{O}$ for the last glacial period in Fukugaguchi Cave most likely resulted from ^{18}O -depleted surface water, which developed in the isolated Japan Sea. The estimated amplitude of the $\delta^{18}\text{O}$ decrease in surface water was ~3‰ at most, consistent with the abnormally low values for foraminifera (by ~2.5‰) in sediment during the last glacial period, shown by samples collected from the Japan Sea. This is the first terrestrial evidence of ^{18}O depletion in Japan Sea surface water during the last glacial period.

Keywords: Stalagmite paleoclimatology, East Asian winter monsoon, Last glacial period, Japan Sea, Oxygen isotope ratio

1 Introduction

High-resolution isotopic records of well-dated stalagmites have been used as paleoclimatic archives in a terrestrial setting (e.g., Cheng et al. 2016). More specifically, the oxygen isotope ($\delta^{18}\text{O}$) records of stalagmites can provide important insight into the precipitation dynamics of the Late Pleistocene and Holocene epochs

and have become a standard proxy for terrestrial climatic changes at the global scale. As a prominent example, Chinese cave records demonstrate that changes in stalagmite calcite $\delta^{18}\text{O}$ ($\delta^{18}\text{O}_\text{C}$) are strongly correlated with $\delta^{18}\text{O}$ records from Greenland ice cores (Wang et al. 2001) and shifts in Northern Hemisphere summer insolation on orbital timescales (Cheng et al. 2016; Wang et al. 2008).

The link between climate and $\delta^{18}\text{O}_\text{C}$ has been mostly attributed to variability in the $\delta^{18}\text{O}$ values of local meteoric water. A popular interpretation is that this results

* Correspondence: akano@eps.s.u-tokyo.ac.jp

¹Department of Earth and Planetary Sciences, Faculty of Science, The University of Tokyo, 7-3-1, Hongo, Bunkyo, Tokyo 113-8654, Japan
Full list of author information is available at the end of the article

from the amount effect on meteoric water $\delta^{18}\text{O}$ ($\delta^{18}\text{O}_\text{w}$) from the intensified East Asian summer monsoon (EASM), which controls the climate in Asia (Cheng et al. 2009; Wang et al. 2001, 2008). Furthermore, $\delta^{18}\text{O}_\text{c}$ is seemingly synchronized with climatic changes in the North Atlantic Ocean during the late Quaternary (Cheng et al. 2016; Sun et al. 2012; Wang et al. 2001, 2008; Zhao et al. 2018). Regarding the warming transition associated with deglaciation from the last glacial period to the mid-Holocene, the stalagmites generally exhibit distinct reductions in $\delta^{18}\text{O}_\text{c}$ values, again ascribed to the intensification of the EASM.

The East Asian winter monsoon (EAWM) is another meteorological system in East Asia (Fig. 1a). The EAWM is driven by the thermal contrast between the Asian continent and the North Pacific during winter, which blows dry and cold northerly winds from the Siberian High (Tada et al. 2016). The EAWM affects the climate of

East Asia (Porter and An 1995) and transports heat from the Northern Hemisphere to the Southern Hemisphere as it crosses the equator (Chu et al. 2017; Yamamoto et al. 2013). EAWM variability during the late Quaternary has been reconstructed using marine sediment cores from the Sulu Sea (de Garidel-Thoron et al. 2001), South China Sea (Huang et al. 2011; Steinke et al. 2010, 2011; Yamamoto et al. 2013), Northwestern Pacific Ocean (Sagawa et al. 2011), and Japan Sea (Nagashima et al. 2007, 2011), as well as from terrestrial archives (e.g., aeolian sediments from the northwestern Chinese Loess Plateau (Sun et al. 2012) and lake sediments in south China (Chu et al. 2017; Yancheva et al. 2007). The $\delta^{18}\text{O}_\text{c}$ rarely reflects the intensity of the EAWM because meteoric water from a dry EAWM makes only a small contribution to total precipitation in East Asia (e.g., An 2000). Exceptional findings were reported in Fukugaguchi Cave at Itoigawa in central Japan, on the coast of the Japan

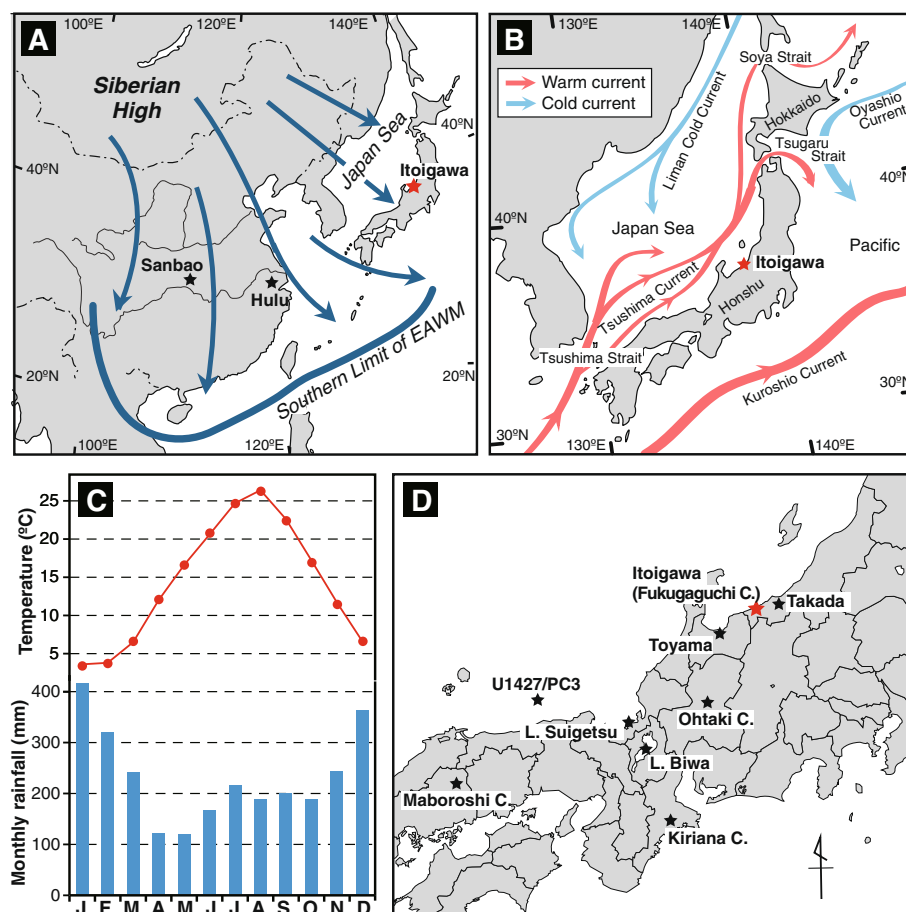


Fig. 1 Geographic and climatological setting of the study site, Itoigawa. **a** Map showing the general wind directions in the winter, the southern limit of the EAWM, and the locations of the Itoigawa and Chinese caves. **b** Warm and cold currents around Japan. The Tsushima Warm Current enters the Japan Sea through the Tsushima strait and outflows to the Northwestern Pacific Ocean through the Tsugaru and Soya straits. **c** Monthly mean temperature (°C) at Itoigawa (upper) and rainfall (mm) at the Hiraiwa Precipitation Observatory (lower) during the period 1990–2009. **d** Locations of caves (Maboroshi, Ohtaki, and Kiriana), lakes (Suigetsu and Biwa), a coring site (U1427/PC3), and observatory sites (Toyama and Takada) discussed in this study

Sea (Sone et al. 2013, 2015), where water vapor from the Japan Sea warmed by the Tsushima Warm Current is carried by a northwesterly of the EAWM from Siberia (Fig. 1b; Hirose and Fukudome 2006). This area is wet in winter, and the snow/rainfall of the winter months (December–February) constitutes $\sim 40\%$ of annual rainfall (Fig. 1c). Considering that the EAWM usually starts in November and ends in March, the EAWM snow/rainfall contributes a larger proportion (it falls 57% of annual rainfall during five months from November to March). Sone et al. (2013) analyzed a Holocene stalagmite (i.e., FG01) from Fukugaguchi Cave (Fig. 1d) and found that $\delta^{18}\text{O}_\text{C}$ variability at the top of FG01 was strongly correlated with that of winter precipitation observed from 1924 to 2010 at Takada (Fig. 1d). On the other hand, the $\delta^{18}\text{O}_\text{C}$ variability did not show relevance to precipitation of other seasons (Sone et al. 2013 in their Fig. 5). The amount effect apparent in $\delta^{18}\text{O}$ values of winter precipitation (collected from Toyama, Fig. 1d) also implied that the $\delta^{18}\text{O}_\text{C}$ reflected winter precipitation variability. In addition, the $\delta^{18}\text{O}_\text{C}$ profile of the entire FG01, covering the past 10 kyr, demonstrated a trend similar to that of EAWM variability reported by other studies on loess and lake sediments (Sone et al. 2013). However, the variability of the EAWM beyond the pre-Holocene period has never been demonstrated based on a stalagmite record. Such data may provide insight regarding the hydroclimate during glacial periods.

Here, we present a new $\delta^{18}\text{O}_\text{C}$ profile spanning the last glacial period from 32.2 to 22.3 ka, obtained from another stalagmite (FG02) in Fukugaguchi Cave. A drastic shift in oceanographic conditions occurred during the last glacial period in the Japan Sea, the major moisture source in the study area. The Japan Sea is currently connected to the open ocean via four shallow straits (Fig. 1b). However, during glacial periods, the lowered sea level largely restricted entry of the Tsushima Warm Current. Freshwater influx from the surrounding land area reduced surface water salinity in the Japan Sea, as indicated by unusually low $\delta^{18}\text{O}$ in foraminifers (Oba et al. 1991; Sagawa et al. 2018). Closing and opening of the Japan Sea led to glacial–interglacial contrast in the compositions and structures of core sediments recovered from the Japan Sea, which are generally laminated during glacial and bioturbated during interglacials (e.g., Irino et al. 2018; Tada et al. 2018; Seki et al. 2019). The closure of the Japan Sea may also have affected the hydrodynamics of vapor generation during glacial periods. Such changes, as well as the intensity of the EAWM and the EASM, may lead to differences in the $\delta^{18}\text{O}_\text{C}$ in FG02 from other cave records in Japan (Maboroshi, Ohtaki, and Kiriana; Fig. 1d), where

precipitation from the EAWM is minor. Moreover, the $\delta^{18}\text{O}_\text{C}$ profile of FG02 exhibits millennial-scale changes that might correspond to climatic changes in the North Pacific Ocean. In this paper, the $\delta^{18}\text{O}_\text{C}$ records from Fukugaguchi Cave are discussed as new stalagmite evidence for the development of ^{18}O -depleted surface water in the Japan Sea during the last glacial period.

2 Materials and methods

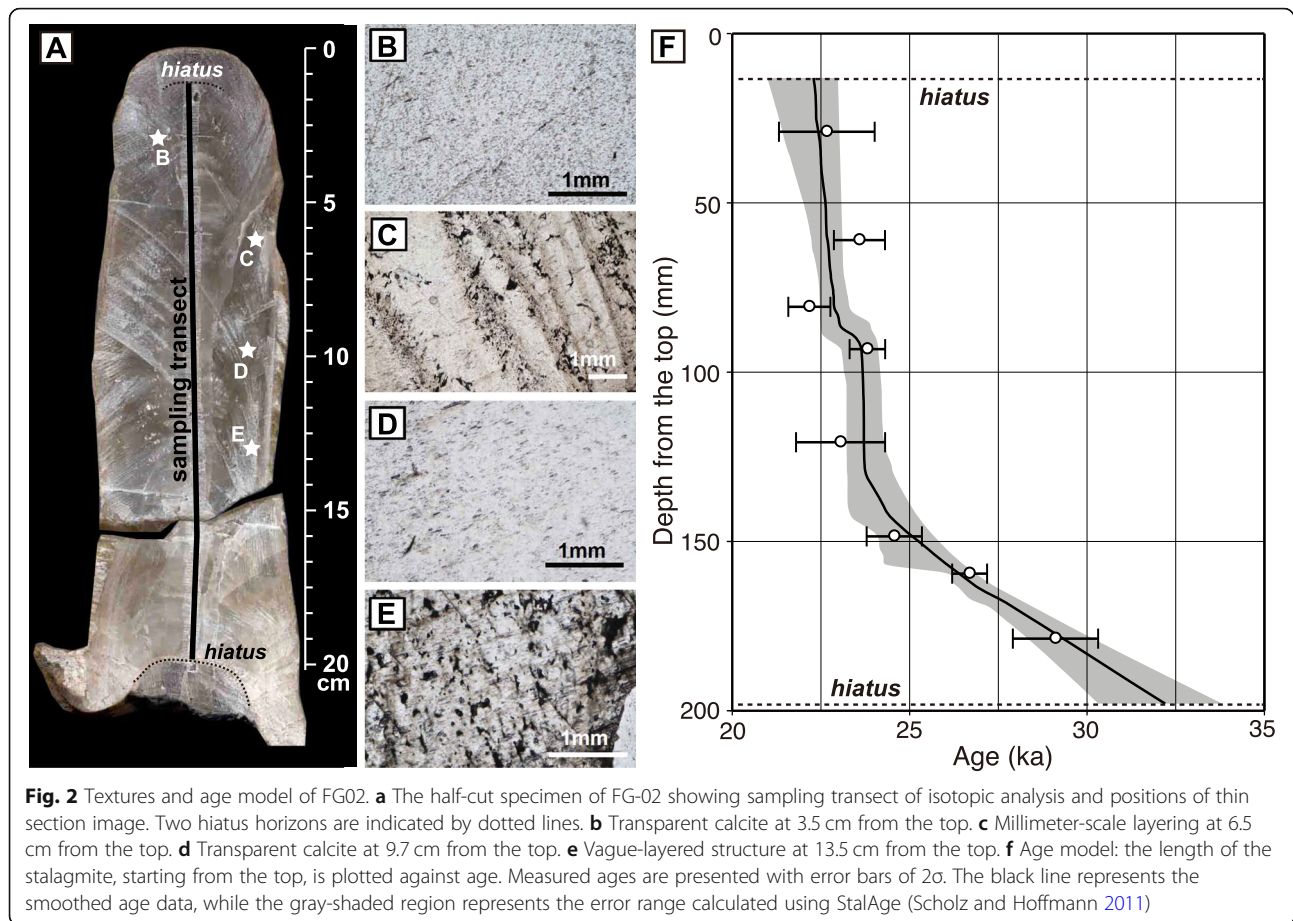
2.1 Study site and stalagmite sample

Fukugaguchi Cave ($36^\circ 96.5' \text{ N}$, $137^\circ 80.0' \text{ E}$) is located in Itoigawa City, Niigata Prefecture, on the coasts of Japanese islands along the Japan Sea (Fig. 1). Itoigawa currently experiences some of the heaviest snowfall in Japan because of its geographic and altitudinal position, i.e., on a steep slope behind high mountains (e.g., Mt. Asahidake, 2418 m asl). A northwesterly of the EAWM reaches this location across the widest breadth of the Japan Sea, where the Tsushima Warm Current supplies water vapor to the initially dry northwesterly (Fig. 1a, b). The wet air mass then interacts with the mountain slope, causing heavy snowfalls. Therefore, the 5-month period (November–March) under the influence of the EAWM is generally wet in this area, accounting for 59% of the annual precipitation in Itoigawa (Sone et al. 2013).

Our sample analyzed in this study was a 22-cm-long stalagmite (FG02; Fig. 2a) collected from Fukugaguchi Cave in 2010. The sampling point was approximately 700 m from the cave entrance and near the location of the Holocene sample (FG01; Sone et al. 2013, 2015), where relative humidity (RH) is nearly 100%. FG02 has two discontinuous surfaces at 13.0 and 198.0 mm from the top (hiatus in Fig. 2a). The stalagmite lacks the regular laminae (Fig. 2b–e) that may constitute annual bands. It mainly consists of transparent calcite mass (Fig. 2b, d), although some distal parts of the stalagmite exhibit mm-scale layering (Fig. 2c, e).

2.2 U–Th age measurement

The ages of FG02 were determined by U–Th dating carried out at the National Taiwan University. The methods were described in detail by Shen et al. (2002, 2003, 2012). The stalagmite was cut along its growth axis for polishing and then drilled at nine horizons along the growth lines. Nine 0.2–0.3-g subsamples were obtained for each analysis. Because of the low uranium concentration in FG02, the amount of each sample was more than twofold greater than the amount used in ordinary U–Th dating (approximately 0.1 g; Shen et al. 2012). These powdered samples were dissolved with 5% nitric acid and spiked with an artificial radiometric tracer (^{229}Th – ^{233}U – ^{236}U). An Fe^{3+} solution was added to this solution to remove Ca^{2+} by iron co-precipitation. U and Th were purified by anion exchange chromatography.



The isotopic signature of each purified fraction was measured with a multicollector inductively coupled plasma mass spectrometer (Neptune; Thermo). An age–depth model was constructed using StalAge software, by means of a statistical algorithm based on Bayesian Monte Carlo simulation (Scholz and Hoffmann 2011).

2.3 Stable isotope analysis

Stable isotope analysis was performed with an isotope ratio mass spectrometer (DeltaPlus; Thermo Finnigan) connected to an online gas separation and introduction system (GasBench II) at Kyushu University. Subsampling was conducted down the middle of the growth band along the growth axis with a dental microdrill (Tas-35LX; Shofu) at 0.2-mm intervals. In addition, a Hendy test to examine the stability of $\delta^{18}\text{O}$ values along specific growth bands (Hendy 1971) was performed for 8–10 subsamples at three horizons. Each ~ 0.15 -mg sample was enclosed in a 12-mL vial. Following replacement with He gas, these subsamples were reacted with phosphoric acid for > 5 h in a 50°C thermostat chamber. Generated CO_2 was introduced to the analysis system. $\delta^{18}\text{O}$ values were normalized by using an in-house standard, which corresponded to the Vienna Pee Dee

Belemnite standard. The reproducibility of the measurements of in-house standard ($N = 190$) was $\pm 0.14\text{‰}$ (2 SD). A typical measuring error is $\pm 0.2\text{‰}$ (2 σ). Additional details of $\delta^{18}\text{O}$ measurement were described by Hori et al. (2009).

2.4 Evaluation of the amount effect of winter precipitation

For the Holocene stalagmite (FG01), Sone et al. (2013) concluded that the variability of $\delta^{18}\text{O}_\text{C}$ largely reflected the intensity of winter precipitation, consistent with the negative correlation between $\delta^{18}\text{O}_\text{W}$ and the amount of rain containing meteoric water during winter. We quantified this amount effect by using a bootstrap method and $\delta^{18}\text{O}_\text{W}$ data collected at Toyama, approximately 60 km southwest of the cave (Fig. 1d). The $\delta^{18}\text{O}_\text{W}$ data included 78 meteoric rain/snow events in winter months (December–February) from 2010 to 2012, which were collected by Sone et al. (2013). A virtual set of winter precipitation data consisted of a given number (N) of rainfall events, which were randomly selected from among the 78 events. First, the range of N was set at 24–30, which reproduced the distribution of total winter precipitation for the last 50 years at Toyama. Then, the

total amount and weighted mean of $\delta^{18}\text{O}_w$ were calculated for each virtual set. For each of seven cases of N (24–30), the selection of virtual sets was repeated 100 times, such that the total number in the virtual set was 700.

3 Results

3.1 Dating result and age–depth model

U–Th dating for FG02 yielded suitable ages from nine horizons, which ranged from ca. 13 to ca. 29 ka (Table 1). Although each age from the nine horizons exhibited relatively large uncertainty, due to the low uranium concentration (typically 6.0 ppb) and relatively high ^{232}Th (e.g., 3820 ppt at 9.5 mm horizon), they were generally in the correct stratigraphic order (Table 1). A distinctly younger age (ca. 13 ka) was obtained from the uppermost dated horizon (10 mm from the top; Table 1, and above the upper hiatus; Fig. 2a). An approximately 10-kyr age difference between this horizon and the next dated horizon (ca. 23 ka) at 30 mm likely signified a hiatus at an upper discontinuous surface (13.0 mm). Another hiatus was suspected at a lower discontinuous surface (198.0 mm), although no reliable age was obtained below this surface. The age model generated with StalAge (Scholz and Hoffmann 2011) indicated that the middle section between the two hiatuses was formed between ca. 32.2 ka and ca. 22.3 ka. The age–depth relation shown in Fig. 2 implies that the growth rate was fast above 130 mm (approximately 45 mm/kyr for 22–24 ka) and slow below 130 mm (approximately 7 mm/kyr for 24–32 ka).

3.2 Stable isotope analysis

The $\delta^{18}\text{O}_C$ values of the middle section of FG02 ranged from -7.48‰ to -10.68‰ , with a mean value of -8.87‰ . This was clearly lower than the range observed in Holocene FG01 (mainly -8.5‰ to -7.0‰ ; Sone et al. 2013, 2015). The $\delta^{18}\text{O}_C$ values of FG02 indicated millennial-scale changes resembling the changes in the paleoclimatic records of the last glacial period. From 32.2 ka (i.e., the bottom) to ca. 26 ka, the $\delta^{18}\text{O}_C$ variability showed sawtooth-shaped fluctuation on a millennial scale (Fig. 3). The fluctuation amplitude was 0.5‰ – 1.0‰ , clearly greater than the $\delta^{18}\text{O}_C$ measurement deviation ($\pm 0.14\text{‰}$). The upper $\delta^{18}\text{O}_C$ profile in the interval from 26 to 24 ka was nearly flat around -9‰ ; this was followed by a positive shift to -8‰ at 23.1 ka, which rapidly recovered at ca. 22.8 ka (Fig. 3).

The results of Hendy tests conducted at 26-, 60-, and 120-mm horizons are shown in Fig. 4a. The mean value was -8.43‰ at 26 mm, -8.79‰ at 60 mm, and -9.28‰ at 120 mm. The three horizons exhibited perturbation within $\pm 0.25\text{‰}$, which was slightly larger than the measurement error of $\delta^{18}\text{O}_C$ ($2\sigma < \pm 0.2\text{‰}$; Fig. 4a). The

covariance between $\delta^{18}\text{O}_C$ and $\delta^{13}\text{C}$ was not confirmed ($R = 0.04$; Fig. 4b), presumably supporting the absence of significant isotopic non-equilibrium.

3.3 Relationship between $\delta^{18}\text{O}$ and winter precipitation at Toyama

A weak negative correlation between the total winter precipitation and weighted mean of $\delta^{18}\text{O}$ was observed upon analysis of 78 meteoric water samples during winter months (December–February) at Toyama (Fig. 5) (Sone et al. 2013). In the past 50 years (1969–2018), 395.5–994.5 mm of rain and snow (mean, 696.4 ± 135 mm) fell each winter (Fig. 5a). First, we reproduced this observed distribution of total winter precipitation by random selection of a range of N (number of rain/snow events) from among the 78 actual events. The closest distribution was obtained with the range of N from 24 to 30 (mean, 687.9 ± 132 mm) (Fig. 5a). The calculation was repeated 100 times for each case of N (24–30; 7 cases), and the 700 virtual sets of winter precipitation data yielded weighted $\delta^{18}\text{O}_C$ values ranging from -10.74‰ to -7.81‰ (mean, $-9.34\text{‰} \pm 0.49\text{‰}$). The precipitation amount and weighted mean (Fig. 5b) indicated a weak but significant negative correlation ($R = -0.33$, $p = 6 \times 10^{-19}$), with a slope of $-1.2\text{‰}/1,000$ mm. We use this slope as the amount effect of modern winter precipitation in the following section.

4 Discussion

4.1 Millennial-scale changes in FG02

The FG02 stalagmite recorded millennial-scale changes according to the characteristic features in the paleoclimatic records during the last glacial period. Figure 6 compares the FG02 $\delta^{18}\text{O}_C$ with the $\delta^{18}\text{O}$ and Ca^{2+} concentration of a Greenland ice core (Rasmussen et al. 2014; Seierstad et al. 2014), as well as a reconstructed EAWM derived from grain size variation in the Chinese Loess Plateau (Sun et al. 2012), and a reconstructed EASM derived from stalagmites in Sanbao and Hulu Caves in China (Wang et al. 2001) and stalagmites in Kiriana Cave on the Pacific Ocean side of Japan (Mori et al. 2018). The FG02 stalagmite shows millennial-scale changes in $\delta^{18}\text{O}_C$. Because the low uranium content of FG02 yields U–Th ages with relatively large uncertainty (Table 1), two possible relationships exist between the $\delta^{18}\text{O}_C$ and Dansgaard–Oeschger (D–O) events (cases 1 and 2; Fig. 6). In order to determine which case is true, stalagmite samples with small uncertainty of U–Th ages are needed.

In case 1, the $\delta^{18}\text{O}_C$ values of FG02 are presumed to be heavier during the D–O interstadials. Three positive $\delta^{18}\text{O}_C$ excursions, at 23.1, 27.3, and 28.7 ka, are correlated with D–O events 2, 3, and 4, respectively (Fig. 6c). Another positive excursion around 30.8 ka is also recognized in the Greenland ice core and Chinese loess

Table 1 Uranium and thorium isotopic compositions and ^{230}Th ages (before 1950 AD) for subsamples of stalagmite FG02 by MC-ICP-MS

Horizon (mm)	Weight (g)	^{238}U (ppb)	^{232}Th (ppt)	$\delta^{234}\text{U}$ (measured) ^a	$^{230}\text{Th}/^{238}\text{U}$ (activity) ^c	$^{230}\text{Th}/^{232}\text{Th}$ (ppm) ^d	Age (uncorrected)	Age (corrected) ^{c,e}	$\delta^{234}\text{U}_{\text{initial}}$ (corrected) ^b
9.5	0.2257	6.01 ± 0.00	3818 ± 13.4	387.7 ± 2.4	0.2987 ± 0.0129	7.8 ± 0.3	26165 ± 1265	13537 ± 6838	402.8 ± 8.0
29.0	0.2416	9.33 ± 0.01	1247 ± 4.2	423.9 ± 2.2	0.2957 ± 0.0056	36.5 ± 0.7	25126 ± 530	22665 ± 1349	452.0 ± 2.9
61.0	0.2635	8.21 ± 0.01	543 ± 2.9	407.2 ± 3.1	0.2889 ± 0.0039	72.1 ± 1.0	24810 ± 377	23585 ± 720	435.2 ± 3.4
80.7	0.2880	7.78 ± 0.02	446 ± 2.6	436.7 ± 3.9	0.2778 ± 0.0030	80.0 ± 1.0	23213 ± 283	22173 ± 593	465.0 ± 4.2
93.2	0.2944	6.32 ± 0.03	293 ± 2.4	443.8 ± 7.1	0.2948 ± 0.0027	105.1 ± 1.2	24642 ± 282	23809 ± 501	474.7 ± 7.6
120.7	0.3347	6.08 ± 0.03	754 ± 4.2	430.8 ± 8.1	0.2993 ± 0.0053	39.8 ± 0.7	25323 ± 524	23053 ± 1255	459.8 ± 8.8
148.5	0.2848	6.07 ± 0.03	431 ± 2.8	483.1 ± 8.9	0.3159 ± 0.0048	73.4 ± 1.2	25812 ± 472	24567 ± 779	517.8 ± 9.6
159.5	0.2749	6.32 ± 0.04	233 ± 2.6	494.0 ± 11.4	0.3349 ± 0.0032	149.9 ± 2.0	27329 ± 381	26691 ± 492	532.8 ± 12.4
178.7	0.2364	5.80 ± 0.04	669 ± 4.1	484.4 ± 10.9	0.3733 ± 0.0064	53.5 ± 0.9	31127 ± 660	29111 ± 1202	525.9 ± 12.0

^a $^{234}\text{U} = ((^{234}\text{U}/^{238}\text{U}) \text{ activity} - 1) \times 1000$.^b $^{234}\text{U}_{\text{initial}}$ corrected was calculated based on ^{230}Th age (T), i.e., $^{234}\text{U}_{\text{initial}} = ^{234}\text{U}_{\text{measured}} \times e^{234\lambda T}$, and T is corrected age^c $^{230}\text{Th}/^{238}\text{U}$ activity = $1 - e^{-230\lambda T} + (^{234}\text{U}_{\text{measured}}/1000)[^{230}\text{Th}/(^{230}\text{Th} - ^{234}\text{U})](1 - e^{-(230-234)\lambda T})$, where T is the age. Decay constants are 9.1577×10^{-6} year⁻¹ for ^{230}Th , 2.8263×10^{-6} year⁻¹ for ^{234}U (Cheng et al. 2013), and 1.55125×10^{-10} year⁻¹ for ^{238}U (Jaffey et al. 1971)^dThe degree of detrital ^{230}Th contamination is indicated by the $^{230}\text{Th}/^{232}\text{Th}$ atomic ratio instead of the activity ratio^eAge corrections were calculated using an estimated atomic $^{230}\text{Th}/^{232}\text{Th}$ ratio of 4 ± 2 ppm

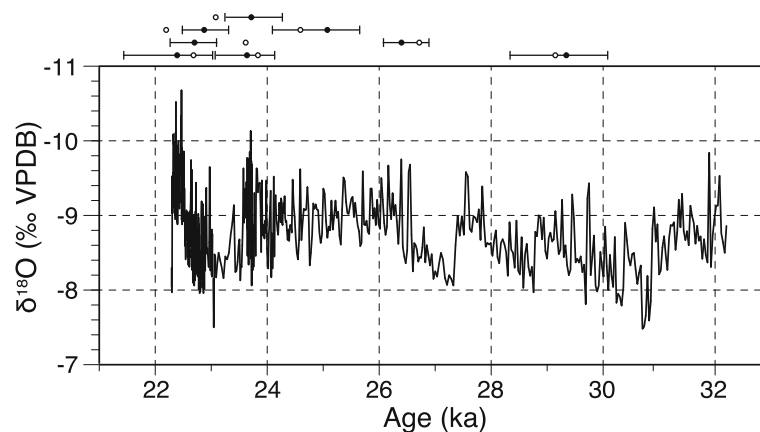


Fig. 3 $\delta^{18}\text{O}_C$ age profile of FG02. Note the inverted vertical axis. Dating results are shown at the top; open circles for the corrected ^{230}Th ages (Table 1), solid circles, and bars for the smoothed ages and the error ranges (Fig. 2), respectively

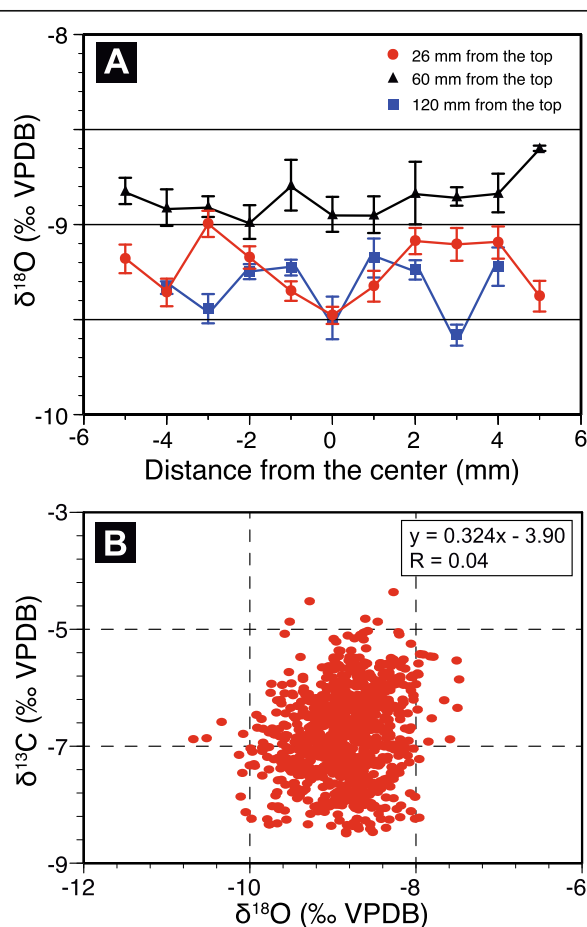
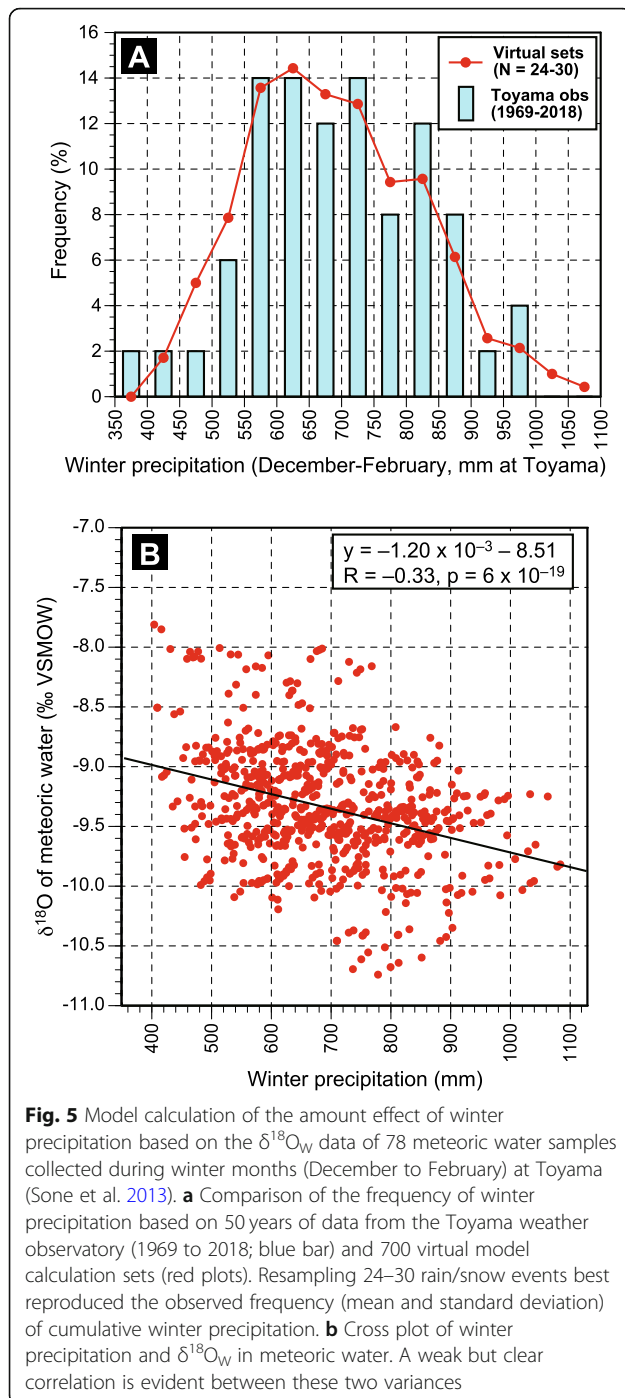


Fig. 4 Isotopic behaviors of FG02. **a** Hendy test results for $\delta^{18}\text{O}_C$ at three growth lines, 26 mm (red), 60 mm (black), and 120 mm (blue) from the top. Subsamples were collected at 1-mm intervals from the central growth axis. **b** Covariance between $\delta^{18}\text{O}$ and $\delta^{13}\text{C}$

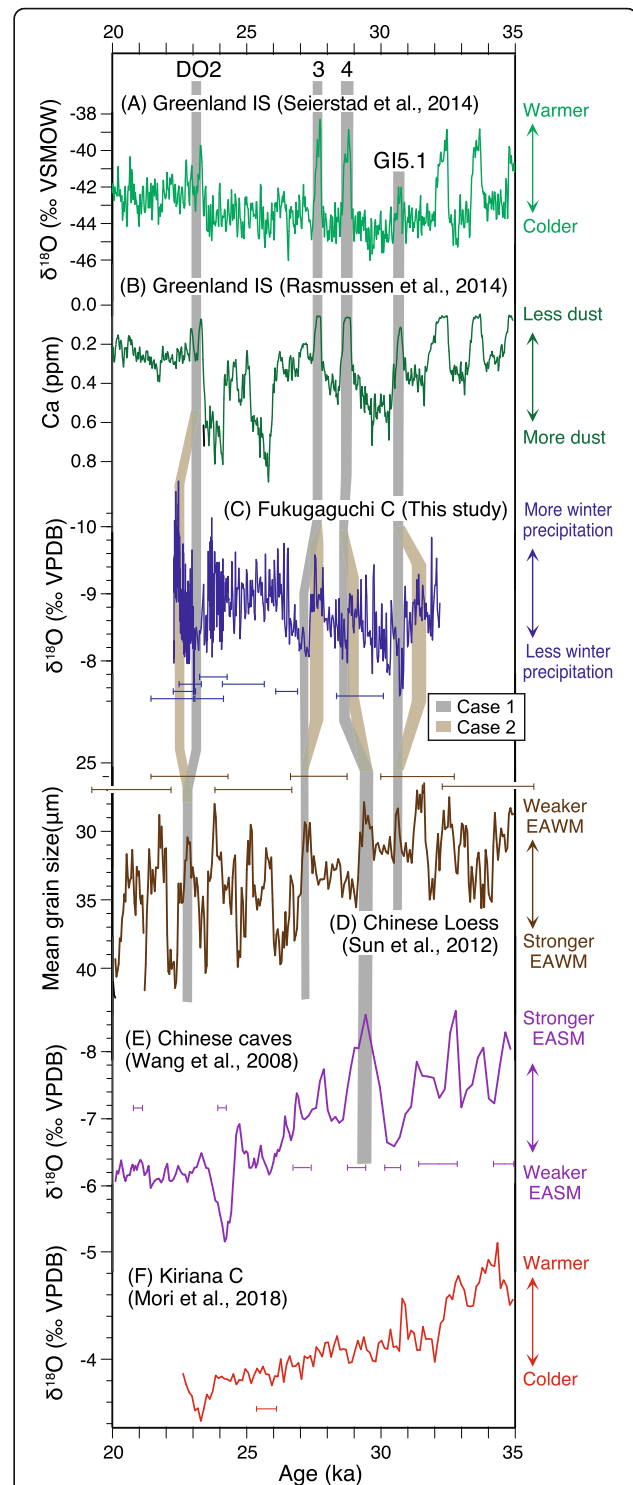
(Fig. 6) and could correspond to the Greenland Interstadial 5.1 (at 30.84 ka) described by Rasmussen et al. (2014). Furthermore, Sone et al. (2013, 2015) concluded that the variability of $\delta^{18}\text{O}_C$ in Holocene FG01 reflects the amount of winter precipitation. According to this interpretation, the millennial-scale positive excursions of $\delta^{18}\text{O}_C$ in FG02 (with an amplitude of 0.5‰–1‰) should have been associated with less winter precipitation and the EAWM during short-term interstadials in Greenland and the North Atlantic Ocean. There might be a linkage between the D–O events and the weakened EAWM, which enriched ^{18}O of meteoric water and FG02.

The $\delta^{18}\text{O}_C$ values of FG02 are presumed to be lighter during the D–O interstadials in case 2. In this scenario, four low- $\delta^{18}\text{O}_C$ intervals at 22.4, 27.6, 29.0, and 31.4 ka correspond to D–O events 2, 3, 4, and 5.1, respectively (Fig. 6c). This scenario fully accords with the stalagmites from China (e.g., Wang et al. 2008), whereby the amount effect due to the intensified EASM reduced $\delta^{18}\text{O}_C$ values during D–O interstadials. However, this is inconsistent with the findings of Sone et al. (2013), suggesting that the variability of the EASM did not strongly affect the stalagmite $\delta^{18}\text{O}_C$. In addition, the $\delta^{18}\text{O}_C$ reduction during these D–O interstadials is unclear even in Kiriana Cave on the Pacific Ocean side of the Japanese islands (Fig. 6f; Mori et al. 2018), where the majority of meteoric water originated from the EASM.

The relationship in case 1 is likely to be more plausible than the relationship in case 2; the $\delta^{18}\text{O}_C$ values of FG02 increased during the D–O events, which contrasts with the findings in Chinese caves. Stalagmite FG02 exhibits an overall decreasing trend of $\delta^{18}\text{O}_C$ (Fig. 6c), which also contrasts with the Chinese stalagmites (Fig. 6e) and findings in Kiriana Cave (Fig. 6f). The case 1 scenario is consistent with the overall trend of $\delta^{18}\text{O}_C$, as well as the



conclusions of Sone et al. (2013, 2015), whereby the variability of $\delta^{18}\text{O}_C$ reflects the amount of winter precipitation. However, considering the calculated amount effect of the modern meteoric water ($-1.2\text{‰}/1000\text{ mm}$; Fig. 5), a 0.5‰ to 1‰ enrichment of $^{18}\text{O}_C$ was only partly compensated by the weakened winter precipitation. A more robust amount effect during the glacial period could be the cause of high $\delta^{18}\text{O}_C$ in FG02 during the D–O events. Alternatively, high $\delta^{18}\text{O}_C$ values during the D–O events



were also associated with other factors, such as the evaporation of water in the soil or cave, which increases both $\delta^{18}\text{O}_\text{w}$ and $\delta^{18}\text{O}_\text{c}$. Our data do not rule out an evaporation effect during water infiltration from the soil. However, any such evaporation effect in the cave was presumably unimportant at the sampling site deep in the cave (700 m from the entrance), because it only appears to be robust where RH is unstable (Deininger et al. 2012).

4.2 Factors responsible for low $\delta^{18}\text{O}_\text{c}$ in glacial FG02

Figure 7 compares the $\delta^{18}\text{O}_\text{c}$ records of the last glacial period (FG02) and the Holocene (FG01) (Sone et al. 2013) with those from three other Japanese stalagmites in Maboroshi Cave in Hiroshima Prefecture (Hiro-1; Hori et al. 2014; Shen et al. 2010; Kato et al. 2021), and Kiriana and Ohtaki Caves in Mie and Gifu Prefectures, respectively (KA03 and OT02; Mori et al. 2018) (see Fig. 1d for locations). The stalagmite records from Fukugaguchi Cave indicate lower $\delta^{18}\text{O}_\text{c}$ values during the last glacial period (FG02) compared with Holocene values (FG01; Sone et al. 2013). This is a unique feature of Fukugaguchi Cave; such variability is not seen in other Japanese and Chinese caves where the EASM is the major source of meteoric water. The Hiro-1, KA03, and OT02 stalagmites exhibit similar $\delta^{18}\text{O}_\text{c}$ variability, with higher values during the last glacial period and lower values in the Holocene, consistent with the Chinese records (e.g., Sanbao and Hulu Caves; Wang et al. 2001, 2008). Comparing our results from Fukugaguchi Cave with the KA03 records from Kiriana Cave that span the entire FG02, a substantial difference ($> 3\text{‰}$) was apparent in the mid-Holocene value minus the glacial period value ($\Delta^{18}\text{O}_{\text{H-G}}$; $+1.23\text{‰}$ in Fukugaguchi and -1.81‰ in Kiriana Cave; Table 2). The negative $\Delta^{18}\text{O}_{\text{H-G}}$ was used to explain the weakened EASM during the glacial period in Chinese records (e.g., Wang et al. 2001). Mori et al. (2018) challenged the notion of an effect of EASM intensity on $\delta^{18}\text{O}_\text{c}$, suggesting that the variability of $\delta^{18}\text{O}_\text{c}$ was largely controlled by air temperature and $\delta^{18}\text{O}$ in seawater, which constituted the major moisture source on the Pacific Ocean side of the Japanese islands. Thus, the $\Delta^{18}\text{O}_{\text{H-G}}$ value of -1.81‰ at Kiriana Cave can be explained by the lower glacial period temperature that caused an increase in fractionation $\delta^{18}\text{O}$ and by ^{18}O -enriched glacial period seawater that caused an increase in moisture $\delta^{18}\text{O}$. The importance of the temperature effect on the stalagmite $\delta^{18}\text{O}_\text{c}$ was also demonstrated for Hiro-1 in Maboroshi Cave by co-variation of $\delta^{18}\text{O}_\text{c}$ and carbonate clumped isotope (Δ_{47} ; Kato et al. 2021).

The EASM intensity, air temperature, and seawater $\delta^{18}\text{O}$ from the Pacific Ocean are important factors controlling $\delta^{18}\text{O}_\text{c}$ in East Asia. However, none of these factors are considered responsible for the positive (+

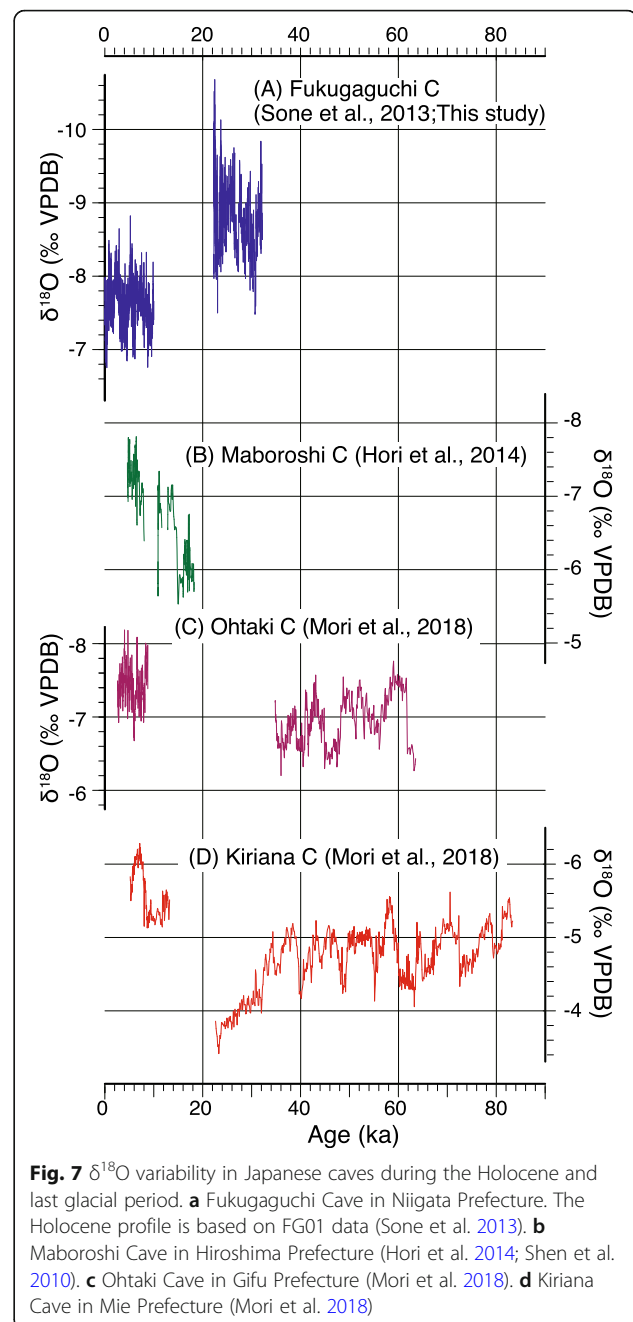


Fig. 7 $\delta^{18}\text{O}$ variability in Japanese caves during the Holocene and last glacial period. **a** Fukugaguchi Cave in Niigata Prefecture. The Holocene profile is based on FG01 data (Sone et al. 2013). **b** Maboroshi Cave in Hiroshima Prefecture (Hori et al. 2014; Shen et al. 2010). **c** Ohtaki Cave in Gifu Prefecture (Mori et al. 2018). **d** Kiriana Cave in Mie Prefecture (Mori et al. 2018)

1.23‰) $\Delta^{18}\text{O}_{\text{H-G}}$ observed at Fukugaguchi Cave. The EASM is a secondary moisture source for Fukugaguchi Cave (Sone et al. 2013, 2015), and EASM weakening is likely to cause negative $\Delta^{18}\text{O}_{\text{H-G}}$. Alkenone-based reconstruction studies for nearshore sediments from the Japan Sea suggested that the sea surface temperature during 17–32 ka was 1–2 °C higher than in the mid-Holocene (Fujine et al. 2006, 2009; Ishiwatari et al. 2001; Xing et al. 2011). Ishiwatari et al. (2001) ascribed these enigmatic results in the Japan Sea to the retention of solar energy on the surface water layer that was stratified with

Table 2 Mean $\delta^{18}\text{O}$ (vs VPDB) during mid-Holocene and the last glacial period recorded in Japanese and Chinese caves

	Middle Holocene		Last glacial		$\Delta^{18}\text{O}_{\text{H-G}}$ (‰)	Reference
	$\delta^{18}\text{O}_{\text{avr}}$ (‰)	Interval (ka)	$\delta^{18}\text{O}_{\text{avr}}$ (‰)	Interval (ka)		
Fukugaguchi	− 7.64	4.2–8.2	− 8.87	22–33	+ 1.23	This study, Sone et al. (2013)
Maboroshi	− 7.29	4.5–8.2	− 6.16	16.0–18.2	− 1.13	Hori et al. (2013)
Kiriana	− 5.94	4.3–8.2	− 4.13	22–33	− 1.81	Mori et al. (2018)
Ohtaki	− 7.37	4.2–8.2	− 6.72	34.8–36	− 0.65	Mori et al. (2018)
Sambo/Hulu ^a	− 10.43	4.2–8.2	− 8.18	22–33	− 2.25	Wang et al. (2001, 2008)

^aCollected more positive (+ 1.9 ‰) Hulu value against Sambo value (Wang et al. 2008)

heavier, deeper layers. Other studies have suggested that diminished salinity during the last glacial period might have led to a change in alkenone production, resulting in a higher reconstructed temperature (Fujine et al. 2006, 2009). Although this interpretation cannot be ruled out, the air temperature on the land was generally lower during the glacial period than the interglacial period, as indicated by pollen assemblages from Lakes Suigetsu and Biwa (Nakagawa et al. 2006, 2008). Similar to other Japanese cave sites, the lower air temperature during the last glacial period would increase $\delta^{18}\text{O}_\text{C}$, thus making $\Delta^{18}\text{O}_{\text{H-G}}$ negative.

With respect to the Holocene $\delta^{18}\text{O}_\text{C}$ variability at Fukugaguchi Cave (FG01), Sone et al. (2013, 2015) considered the intensity of the EAWM and winter precipitation to be dominant factors. The correlation between $\delta^{18}\text{O}_\text{C}$ and winter (December–February) precipitation at Takada (Fig. 1d) is evident in high-resolution $\delta^{18}\text{O}_\text{C}$ analysis of the uppermost FG01, with a 1‰ difference between the dry (1000 mm/3 months) winters in the late 2000s and wet (1500 mm/3 months) winters in the early 1940s at Itoigawa (Sone et al. 2013). Additionally, our analysis of data from Toyama, which is a drier area, revealed a negative correlation of $\delta^{18}\text{O}_\text{W}$ with the amount of precipitation (slope of $-1.2\text{‰}/1,000\text{ mm}$ (Fig. 5b)). In this scenario, a stronger EAWM during the last glacial period (Huang et al. 2011; Steinke et al. 2010; Tian et al. 2010) substantially increased winter precipitation (thus decreasing $\delta^{18}\text{O}_\text{W}$) and generated an approximately 3‰ difference in $\Delta^{18}\text{O}_{\text{H-G}}$ between the Japan Sea side (+ 1.23‰ at Fukugaguchi Cave) and the Pacific Ocean side of the islands (− 1.81‰ at Kiriana Cave; Table 2). When the slope of $-1.2\text{‰}/1000\text{ mm}$ is regarded as the amount effect of the winter precipitation, the $\sim 3\text{‰}$ difference requires 2500 mm of winter precipitation during the glacial period, which is more than fourfold greater than the present amount of winter precipitation at Toyama. However, such a large amount of winter precipitation is considered unrealistic because the pollen records from Lakes Suigetsu (Nakagawa et al. 2006) and Biwa (Hayashi et al. 2010) suggest drier winter conditions during the same period. Furthermore, Schlolaut et al. (2014) suggested that the winter monsoon on the

Japan Sea coast had less moisture during the glacial period because of the limited inflow of the Tsushima Warm Current.

If conditions on the sea surface were drier, the enhanced fractionation from water to vapor could generate lower $\delta^{18}\text{O}$ in both water vapor and stalagmites (Lachniet 2009). The effect of RH on the $\delta^{18}\text{O}$ in water vapor has been estimated in several studies; a 10% reduction in RH was posited to decrease the vapor $\delta^{18}\text{O}$ by 1.3‰ (Gonfiantini 1986) and, in another study, by 0.6‰ (Merlivat and Jouzel 1979). Considering these contrasting estimates, the $\sim 3\text{‰}$ difference corresponds to a 25–50% decrease in RH on the Japan Sea side, whereas the RH has remained stable on the Pacific Ocean side. However, this scenario might reduce winter precipitation, causing the meteoric water at Itoigawa to be dominated by summer precipitation that is more ^{18}O -rich than winter precipitation (Sone et al. 2013). Therefore, the RH effect is unlikely to be equivalent to an approximately 3‰ difference.

A factor likely to be important in the positive $\Delta^{18}\text{O}_{\text{H-G}}$ at Fukugaguchi Cave is the change in $\delta^{18}\text{O}_{\text{SW}}$ on the surface of the Japan Sea (i.e., the dominant vapor source for the cave) (Sone et al. 2013). Currently, $\delta^{18}\text{O}_{\text{SW}}$ is comparable between the Japan Sea and the Pacific Ocean. The Japan Sea is a landlocked marginal sea that connects with the East China Sea and the Pacific Ocean through four narrow straits (Fig. 1b). Because all four straits are shallow, water exchange (e.g., inflow of the Tsushima Warm Current) was largely limited during the last glacial maximum when sea level was reduced by $\sim 130\text{ m}$ (Matsui et al. 1998). Under this restricted condition, the surface seawater may have been diluted by riverine water from the Russian mainland and Japanese islands. Sediment cores from the Japan Sea indicate strong stratification during the last glacial period (Oba et al. 1991; Sagawa et al. 2018), which consisted of oxygen-deficient deep water and low-salinity surface water (Tada et al. 1992, 1999). ^{18}O depletion of the Japan Sea surface was first proposed because of the unusually low $\delta^{18}\text{O}$ in planktonic foraminifera during the last glacial period, recorded in sediment cores recovered from a depth of 935 m at Oki Ridge (Oba et al. 1991) and 800–750 m offshore of Akita (Okumura et al. 1996). By using $\delta^{18}\text{O}$

records of planktonic foraminifera (*Globigerina umbilicate*; Oba et al. 1995) and assuming $\delta^{18}\text{O}_\text{W}$ in the modern freshwater inflow to the Japan Sea (-7.6‰), Matsui et al. (1998) estimated that the $\delta^{18}\text{O}_\text{W}$ in the Japan Sea surface water fell to 20‰ during the last glacial maximum. This drastic decrease in salinity is conceivable if the significant sea-level fall during the last glacial maximum led to reduced seawater inflow through the Tsushima Strait (Matsui et al. 1998). The development of the ^{18}O -depleted water mass during the last glacial period was recently confirmed by higher-resolution data of foraminifera $\delta^{18}\text{O}$ obtained from marine sediments drilled at a shallower depth (330 m at IODP site U1427/PC3; Sagawa et al. 2018). At this site, both benthic (*Uvigerina* spp. and *Cassidulina* spp.) and planktonic foraminifera (*Globigerina bulloides*) began to exhibit decreasing $\delta^{18}\text{O}$ from ca. 32 ka to the last glacial maximum, then showed increasing $\delta^{18}\text{O}$ at ca. 12 ka (Fig. 8; Sagawa et al. 2018). The amplitude of this negative anomaly, compared with the Pacific Ocean standard (Lisiecki and Stern 2016), is approximately

2.5‰ and has been attributed to decreased $\delta^{18}\text{O}_\text{SW}$ on the surface of the Japan Sea (Sagawa et al. 2018). Because the surface water of the Japan Sea is the major moisture source for the Fukugaguchi Cave, the anomalous ^{18}O depletion could have reduced the $\delta^{18}\text{O}$ in meteoric water and stalagmites. Considering the 2.5‰ depletion of $\delta^{18}\text{O}_\text{SW}$ at the coring site (330-m depth), greater depletion was suspected at the sea surface. This might be the dominant factor driving the 3‰ difference of $\Delta^{18}\text{O}_\text{H-G}$. The $\delta^{18}\text{O}_\text{C}$ record from FG02 represents the first terrestrial data supporting seawater stratification and ^{18}O depletion during the glacial period in the Japan Sea. Furthermore, it implies stronger stratification in an earlier stage of the last glacial period compared with previous findings. The FG02 $\delta^{18}\text{O}_\text{C}$ values were significantly lower at 32.2 ka, indicating that the ^{18}O -depleted surface water mass had existed prior to 32.2 ka.

The magnitude of the salinity reduction at the sea surface can be estimated using the $\delta^{18}\text{O}_\text{W}$ in freshwater entering the Japan Sea from the surrounding land area.

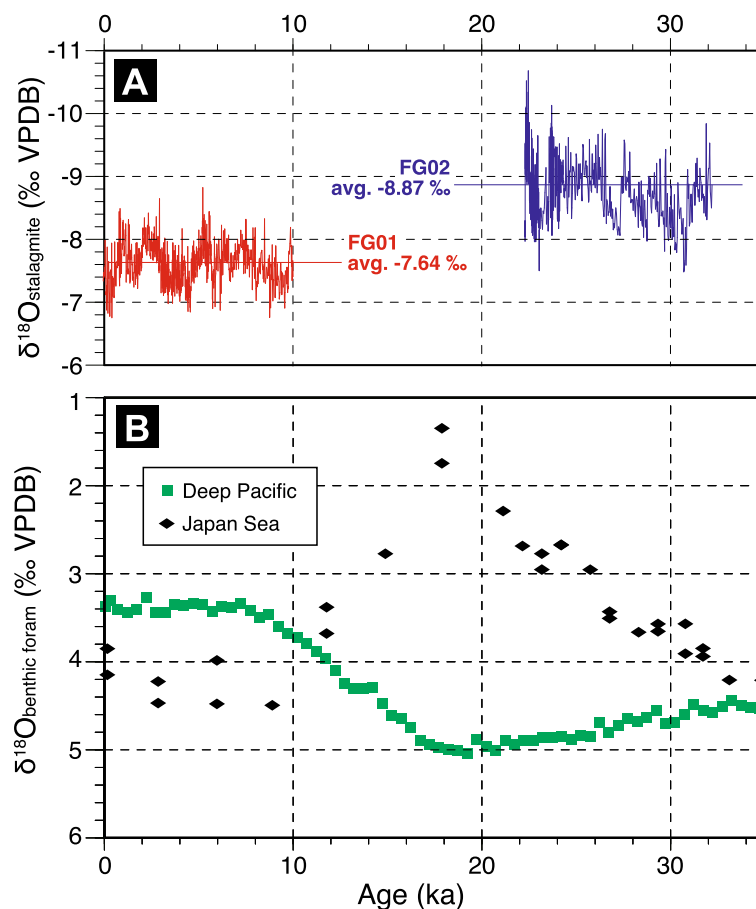


Fig. 8 Isotopic evidence of ^{18}O depletion in the Japan Sea during the last glacial period. **a** $\delta^{18}\text{O}$ in stalagmites from Fukugaguchi Cave (FG01, Sone et al. 2013; FG02, this study). **b** Benthic foraminifera $\delta^{18}\text{O}$ from a coring site at 330 m depth in the Japan Sea (Sagawa et al. 2018) and Northwestern Pacific Ocean (Lisiecki and Stern 2016). Both sets of isotopic data incorporate variability in water $\delta^{18}\text{O}_\text{W}$ and temperature

There are only two Global Networks of Isotopes in Precipitation sites in coastal areas of the Japan Sea: Pohang in South Korea and Terney in Russia. These sites recorded weighted mean meteoric water $\delta^{18}\text{O}$ ($\delta^{18}\text{O}_{\text{MW}}$) values of -7.78‰ in the period 1961–1976 and -9.09‰ in the period 1996–2000, respectively (http://www-naweb.iaea.org/napc/ih/IHS_resources_gnip.html). Considering these data and the weighted mean $\delta^{18}\text{O}_{\text{MW}}$ at Toyama (-9.71‰ ; Sone et al. 2013), the modern mean $\delta^{18}\text{O}_{\text{MW}}$ entering the Japan Sea is estimated to be approximately -9‰ . Here, we define the proportion of freshwater (f_{MW}) in the Japan Sea surface water mass during the glacial period, as well as isotopic values in freshwater ($\delta^{18}\text{O}_{\text{MW}}$), seawater ($\delta^{18}\text{O}_{\text{SW}}$), and the Japan Sea surface ($\delta^{18}\text{O}_{\text{JS}}$), as shown below.

$$\delta^{18}\text{O}_{\text{JS}} = f_{\text{MW}}\delta^{18}\text{O}_{\text{MW}} + (1 - f_{\text{MW}})\delta^{18}\text{O}_{\text{SW}}$$

Assuming that $\delta^{18}\text{O}_{\text{SW}}$ and $\delta^{18}\text{O}_{\text{MW}}$ were $+1\text{‰}$ (Schrug et al. 2002) and -9‰ , respectively, a $2.5\text{--}3.0\text{‰}$ reduction in the Japan Sea surface water ($\delta^{18}\text{O}_{\text{JS}} = -1.5$ to -2.0‰) indicates f_{MW} of $0.25\text{--}0.3$. Assuming glacial period ocean water salinity of 35, the Japan Sea surface salinity ranged from 24.5 to 26.3. This is in the lower part of the salinity range ($24.0\text{--}32.5$) estimated for $22\text{--}32$ ka by Matsui et al. (1998); their estimate was based on $\delta^{18}\text{O}$ in planktic foraminifers (*Globigerina umbilicata*), while ours was based on $\delta^{18}\text{O}$ in the stalagmite. In the closed Japan Sea during the glacial period, the salinity at the sea surface, where vapor is generated, was probably lower than the salinity at the foraminifer habitat depth. In addition to freshwater inflow, sea ice production in the Northern Japan Sea may have contributed to ^{18}O -depletion of the surface water, because frozen water becomes relatively enriched with ^{18}O . Based on the occurrence of dropstones and ice-rafted debris in sediment cores, Ikehara (2003) reconstructed that the sea ice in the northern Japan Sea approached the southern end of Hokkaido during the last glacial maximum. However, ice melting during summer releases ^{18}O -enriched water, and the effect of sea ice development on $\delta^{18}\text{O}_{\text{SW}}$ is not sustainable. Thus, seasonal waxing and waning of sea ice were unlikely to cause a marked reduction in $\delta^{18}\text{O}_{\text{SW}}$. In addition, oxygen isotopic enrichment from water to ice is only $\sim 3\text{‰}$ (O'Neil 1968). Sustainable freshwater influx of -9‰ was presumably a major factor in ^{18}O depletion in the Japan Sea surface water.

A similar linkage between marine and $\delta^{18}\text{O}_{\text{C}}$ records was reported in the eastern Mediterranean (Bar-Matthews et al. 2003), where $\delta^{18}\text{O}_{\text{SW}}$ is sensitive to climatic conditions. Two stalagmite records in Israel extending to 250 ka are consistent with the $\delta^{18}\text{O}_{\text{C}}$ in *Globigerinoides ruber* in the eastern Mediterranean (Fontugne and Calvert 1992).

Both marine and stalagmite $\delta^{18}\text{O}$ showed minimum values during sapropel events (i.e., humid intervals in interglacial period marine isotope stages 5 and 7), which developed under enhanced low-latitude hydrological activity. Currently, the $\delta^{18}\text{O}_{\text{SW}}$ in the eastern Mediterranean is $+1.6\text{‰}$ (Pierre 1999), although this has been reduced by additional meteoric water during humid periods (Kallel et al. 1997). While Bar-Matthews et al. (2003) partly ascribed the low $\delta^{18}\text{O}_{\text{C}}$ values of the stalagmites to the amount effect observed in the area, the reduction of $\delta^{18}\text{O}_{\text{SW}}$ was also an essential factor involved in the low $\delta^{18}\text{O}_{\text{C}}$. Moisture source $\delta^{18}\text{O}_{\text{W}}$ is an essential factor governing stalagmite $\delta^{18}\text{O}_{\text{C}}$.

5 Conclusions

Stalagmite FG02 during the last glacial period ($32.3\text{--}22.3$ ka) in Fukugaguchi Cave on the Japan Sea side of the Japanese islands shows unique $\delta^{18}\text{O}_{\text{C}}$ trends, which have not been previously described in other caves in East Asia. Due to the relatively large uncertainty of U–Th ages, we examined two possible relationships (Fig. 6). The scenario in case 2 contrasts with the findings of a previous Japanese cave study, suggesting that EASM variability did not generate clear $\delta^{18}\text{O}_{\text{C}}$ peaks during D–O interstadials. According to the scenario in case 1, four positive excursions of the $\delta^{18}\text{O}_{\text{C}}$ profile probably correspond to three D–O events and one interval of high $\delta^{18}\text{O}$ in the Greenland ice sheet (Fig. 6). We considered that case 1 correlation was more likely. An important finding of this study was that the glacial FG02 had distinctively lower $\delta^{18}\text{O}_{\text{C}}$ than the Holocene stalagmite from the same cave (FG01). Its mean value (-8.87‰) is 1.23‰ lower than the mid-Holocene mean value ($4.2\text{--}8.2$ ka, -7.64‰ ; Sone et al. 2013). This feature is unique to the Fukugaguchi Cave, i.e., is inconsistent with the $\delta^{18}\text{O}_{\text{C}}$ records from other Japanese and Chinese caves (Fig. 7). The factor making the largest contribution to reduced $\delta^{18}\text{O}_{\text{C}}$ in FG02 was presumably the development of low-salinity water in the semi-isolated Japan Sea, consistent with foraminifera $\delta^{18}\text{O}$ findings (Oba et al. 1991; Sagawa et al. 2018). The amount effect of the intensified EAWM was a potential factor in the seduction in $\delta^{18}\text{O}_{\text{C}}$ in FG02. However, our model calculation based on $\delta^{18}\text{O}_{\text{W}}$ at Toyama indicated that the amount effect of winter precipitation ($1.2\text{‰}/1000$ mm; Fig. 5) was insufficient to explain the observed $2.5\text{--}3.0\text{‰}$ depletion. In addition, the generation of water vapor and winter precipitation likely decreased during the last glacial period due to the blocking of the Tsushima Warm Current. Our stalagmite record provides insight regarding ^{18}O depletion and salinity in the Japan Sea surface water during the last glacial period.

6 Supplementary Information

The online version contains supplementary material available at <https://doi.org/10.1186/s40645-021-00409-8>.

Additional file 1.

Abbreviations

D–O: Dansgaard–Oeschger; EASM: East Asian summer monsoon; EAWM: East Asian winter monsoon

Acknowledgements

We are grateful to Norio Iyota and Yoichi Kamikawa of the Taiheyo Cement Co. for kindly accepting our project and allowing our research in the Fukugaguchi Cave in the limestone mine. We obtained weather data from the website of the Japan Meteorological Agency (<http://www.jma.go.jp/>) and $\delta^{18}\text{O}_w$ data from Global Network of Isotopes in Precipitation (http://www-naweb.iaea.org/naweb/ih/IHS_resources_gnip.html). We would like to thank Engao and Textcheck for the English language review.

Authors' contributions

AK proposed the topic, conceived and designed the study, and supervised SA, KK, TO, and AK obtained the material. SA, MH, TS, HK, TLY, and CCS carried out the experimental work. SA 440 and AK analyzed the data and helped in their interpretation. SA and AK wrote the manuscript of this study with contributions from KK, MH, TLY, and CCS. The authors read and approved the final manuscript.

Funding

This study was financially supported by the JSPS KAKENHI Grant Number JP18J13186 to SA, JP16H02235, and 20H00191 to AK. We are also thankful for the financial support provided by grants from the Science Vanguard Research Program of the Ministry of Science and Technology (MOST) (107-2119-M-002-051, 108-2119-M-002-012), the National Taiwan University (109 L8926), and the Higher Education Sprout Project of the Ministry of Education, Taiwan ROC (108 L901001) to CCS.

Availability of data and materials

The dataset supporting the conclusions of this article is included within the article and its [additional file](#).

Competing interests

The authors declare that they have no competing interests.

Author details

¹Department of Earth and Planetary Sciences, Faculty of Science, The University of Tokyo, 7-3-1, Hongo, Bunkyo, Tokyo 113-8654, Japan. ²Department of Environmental Biology and Chemistry, Faculty of Science, University of Toyama, 3109 Gofuku, Toyama 930-8555, Japan. ³Division of Natural Sciences, Osaka Kyoiku University, 4-698-1, Asahigaoka, Kasiwara City, Osaka 582-8582, Japan. ⁴Marine Works Japan LTD., 3-54-1, Oppamahigashi, Yokosuka 237-0063, Japan. ⁵Center for Advanced Marine Core Research, Kochi University, 200 Monobe Otsu, Nankoku, Kochi 783-8502, Japan. ⁶Center for High-precision Mass Spectrometry and Environment Change Laboratory (HISPEC), Department of Geosciences, National Taiwan University, No. 1, Section 4, Roosevelt Rd, Taipei 10617, Taiwan, ROC. ⁷Global Change Research Center, National Taiwan University, No. 1, Section 4, Roosevelt Rd, Taipei 10617, Taiwan, ROC. ⁸Research Center for Future Earth, National Taiwan University, No. 1, Section 4, Roosevelt Rd, Taipei 10617, Taiwan, ROC.

Received: 28 October 2020 Accepted: 21 January 2021

Published online: 22 February 2021

References

- An Z (2000) The history and variability of the East Asian paleomonsoon climate. *Quat Sci Rev* 19:171–187
- Bar-Matthews M, Ayalon A, Gilmour M, Matthews A, Hawkesworth CJ (2003) Sea–land oxygen isotopic relationships from planktonic foraminifera and speleothems in the Eastern Mediterranean region and their implication for paleorainfall during interglacial intervals. *Geochim Cosmochim Acta* 67:3181–3199
- Cheng H, Edwards RL, Broecker WS, Denton GH, Kong X, Wang Y, Zhang R, Wang X (2009) Ice age terminations. *Science* 326:248–252
- Cheng H, Edwards RL, Shen CC, Polyak VJ, Asmerom Y, Woodhead J, Hellstrom J, Wang Y, Kong X, Spötl C, Wang X, Alexander EC (2013) Improvements in ^{230}Th dating, ^{230}Th and ^{234}U half-life values, and U–Th isotopic measurements by multi-collector inductively coupled plasma mass spectrometry. *Earth Planet Sci Lett* 371:82–91
- Cheng H, Edwards RL, Sinha A, Spötl C, Yi L, Chen S, Kelly M, Kathayat G, Wang X, Li X, Kong X, Wang Y, Ning Y, Zhang H (2016) The Asian monsoon over the past 640,000 years and ice age terminations. *Nature* 534:640–646
- Chu G, Sun Q, Zhu Q, Shan Y, Shang W, Ling Y, Su Y, Xie M, Wang X, Liu J (2017) The role of the Asian winter monsoon in the rapid propagation of abrupt climate changes during the last deglaciation. *Quat Sci Rev* 177:120–129
- de Garidel-Thoron T, Beaufort L, Linsley BK, Dannenmann S (2001) Millennial-scale dynamics of the East Asian winter monsoon during the last 200,000 years. *Paleoceanogr* 16:491–502
- Deininger M, Fohlmeister J, Scholz D, Mangini A (2012) Isotope disequilibrium effects: the influence of evaporation and ventilation effects on the carbon and oxygen isotope composition of speleothems—A model approach. *Geochim Cosmochim Acta* 96:57–79
- Fontugne MR, Calvert SE (1992) Late Pleistocene variability of the carbon isotopic composition of organic matter in the eastern mediterranean: monitor of changes in carbon sources and atmospheric CO_2 concentrations. *Paleoceanogr* 7:1–20
- Fujine K, Yamamoto M, Tada R, Kido Y (2006) A salinity-related occurrence of a novel alkenone and alkenoate in Late Pleistocene sediments from the Japan Sea. *Org Geochem* 37:1074–1084
- Fujine K, Tada R, Yamamoto M (2009) Paleotemperature response to monsoon activity in the Japan Sea during the last 160 kyr. *Palaeogeogr Palaeoclimatol Palaeoecol* 280:350–360
- Gonfiantini R (1986) Environmental isotopes in lake studies. In: Fritz P, Fontes JC (eds) *Handbook of Environmental Geochemistry*, vol 2. Elsevier, Amsterdam, pp 113–168
- Hayashi R, Takahara H, Hayashida A, Takemura K (2010) Millennial-scale vegetation changes during the last 40,000 yr based on a pollen record from Lake Biwa, Japan. *Quat Res* 74:91–99
- Hendy CH (1971) The isotopic geochemistry of speleothems—I. The calculation of the effects of different modes of formation on the isotopic composition of speleothems and their applicability as palaeoclimatic indicators. *Geochim Cosmochim Acta* 35:801–824
- Hirose N, Fukudome K-I (2006) Monitoring the Tsushima warm current improves seasonal prediction of the regional snowfall. *Sci Online Lett Atmos* 2:61–63
- Hori M, Kawai T, Matsuoka J, Kano A (2009) Intra-annual perturbation of stable isotopes in tufas: effects of hydrological processes. *Geochim Cosmochim Acta* 73:1684–1695
- Hori M, Ishikawa T, Nagaishi K, Lin K, Wang BS, You CF, Shen CC, Kano A (2013) Prior calcite precipitation and source mixing process influence Sr/Ca, Ba/Ca and $^{87}\text{Sr}/^{86}\text{Sr}$ of a stalagmite developed in southwestern Japan during 18.0–4.5 ka. *Chem Geol* 347:190–198
- Hori M, Ishikawa T, Nagaishi K, You CF, Huang KF, Shen CC, Kano A (2014) Rare earth elements in a stalagmite from southwestern Japan: a potential proxy for chemical weathering. *Geochim J* 48:73–84
- Huang E, Tian J, Steinke S (2011) Millennial-scale dynamics of the winter cold tongue in the southern South China Sea over the past 26 ka and the East Asian winter monsoon. *Quat Res* 75:196–204
- Ikehara K (2003) Late Quaternary seasonal sea-ice history of the northeastern Japan Sea. *J Oceanogr* 59:585–593
- Irino T, Tada R, Ikehara K, Sagawa T, Karasuda A, Kurokawa S, Seki A, Lu S (2018) Construction of perfectly continuous records of physical properties for dark-light sediment sequences collected from the Japan Sea during Integrated Ocean Drilling Program Expedition 346 and their potential utilities as paleoceanographic studies. *Prog Earth Planet Sci* 5:23
- Ishiwatari R, Houtatsu M, Okada H (2001) Alkenone-sea surface temperatures in the Japan Sea over the past 36 kyr: Warm temperatures at the last glacial maximum. *Org Geochem* 32:57–67
- Jaffey AH, Flynn KF, Glendenin LE, Bentley WC, Essling AM (1971) Precision measurement of half-lives and specific activities of ^{235}U and ^{238}U . *Phys Rev C* 4:1889
- Kallel N, Paterne M, Duplessy JC, Vergnaud-Grazzini C, Pujol C, Labeyrie L, Arnold M, Fontugne M, Pierre C (1997) Enhanced rainfall in the Mediterranean region during the last Sapropel Event. *Oceanologica Acta* 20:697–712
- Kato H, Amekawa S, Hori M, Shen CC, Kuwahara Y, Senda R, Kano A (2021) Influences of temperature and the meteoric water $\delta^{18}\text{O}$ value on a

- stalagmite record in the last deglacial to middle Holocene period from southwestern Japan. *Quat Sci Rev* 53:1667–46
- Lachniet MS (2009) Climatic and environmental controls on speleothem oxygen-isotope values. *Quat Sci Rev* 28:412–432
- Lisiecki LE, Stern JV (2016) Regional and global benthic $\delta^{18}\text{O}$ stacks for the last glacial cycle. *Paleoceanography* 31:1368–1394
- Matsui H, Tafa R, Oba T (1998) Low-salinity isolation event in the Japan Sea in response to eustatic sea-level drop during LGM: reconstruction based on salinity-balance model. *Quat Res (Daiyonkikenkyu)* 37:221–233
- Merlivat L, Jouzel J (1979) Global climatic interpretation of the deuterium-oxygen 16 relationship for precipitation. *J Geophys Res: Ocea* 84:5029–5033
- Mori T, Kashiwagi K, Amekawa S, Kato H, Okumura T, Takashima C, Wu CC, Shen CC, Quade J, Kano A (2018) Temperature and seawater isotopic controls on two stalagmite records since 83 ka from maritime Japan. *Quat Sci Rev* 192:47–58
- Nagashima K, Tada R, Matsui H, Irino T, Tani A, Toyoda S (2007) Orbital- and millennial-scale variations in Asian dust transport path to the Japan Sea. *Paleogeogr Palaeoclimatol Palaeoecol* 247:144–161
- Nagashima K, Tada R, Tani A, Sun Y, Isozaki Y, Toyoda S, Hasegawa H (2011) Millennial-scale oscillations of the westerly jet path during the last glacial period. *J Asian Earth Sci* 40:1214–1220
- Nakagawa T, Tarasov PE, Kitagawa H, Yasuda Y, Gotanda K (2006) Seasonally specific responses of the East Asian monsoon to deglacial climate changes. *Geology* 34:521–524
- Nakagawa T, Okuda M, Yonenobu H, Miyoshi N, Fujiki T, Gotanda K, Tarasov PE, Morita Y, Takemura K, Horie S (2008) Regulation of the monsoon climate by two different orbital rhythms and forcing mechanisms. *Geology* 36:491–494
- Oba T, Kato M, Kitazato H, Koizumi I, Omura A, Sakai T, Takayama T (1991) Paleoenvironmental changes in the Japan Sea during the last 85,000 years. *Paleoceanography* 6:499–518
- Oba T, Murayama M, Matsumoto E, Nakamura T (1995) AMS- ^{14}C ages of Japan Sea cores from the Oki Ridge. *Quat Res (Daiyonkikenkyu)* 34: 289–296
- Okumura S, Minagawa M, Oba T, Ikehara K (1996) Paleoenvironmental analysis of two sediment cores off Akita City in the Japan Sea based on oxygen, carbon and nitrogen isotope. *Quat Res (Daiyonkikenkyu)* 35:349–358
- O'Neil JR (1968) Hydrogen and oxygen isotope fractionation between ice and water. *J Phys Chem* 72:3683–3684
- Pierre C (1999) The oxygen and carbon isotope distribution in the Mediterranean water masses. *Mar Geol* 153:41–55
- Porter SC, An Z (1995) Correlation between climate events in the North Atlantic and China during the last glaciation. *Nature* 375:305–308
- Rasmussen SO, Bigler M, Blockley SP, Blunier T, Buchardt SL, Clausen HB, Cvijanovic I, Dahl-Jensen D, Johnsen SJ, Fischer H, Gkinis V, Guillevic M, Hoek WZ, Lowe JJ, Pedro JB, Popp T, Seierstad IK, Steffensen JP, Svensson AM, Vallelonga P, Vinther BM, Walker MJC, Wheatley JJ, Winstrup M (2014) A stratigraphic framework for abrupt climatic changes during the Last Glacial period based on three synchronized Greenland ice-core records: Refining and extending the INTIMATE event stratigraphy. *Quat Sci Rev* 106:14–28
- Sagawa T, Yokoyama Y, Ikehara M, Kuwae M (2011) Vertical thermal structure history in the western subtropical North Pacific since the Last Glacial Maximum. *Geophys Res Lett* 38:3–7
- Sagawa T, Nagahashi Y, Satoguchi Y, Holbourn A, Itaki T, Gallagher SJ, Saavedra-Pellitero M, Ikehara K, Irino T, Tada R (2018) Integrated tephrostratigraphy and stable isotope stratigraphy in the Japan Sea and East China Sea using IODP Sites U1426, U1427, and U1429, Expedition 346 Asian Monsoon. *Prog Earth Planet Sci* 5:18
- Schlöglaut G, Brauer A, Marshall MH, Nakagawa T, Staff RA, Ramsey CB, Lamb HF, Bryant CL, Naumann R, Dulski P, Brock F, Yokoyama Y, Tada R, Haraguchi T (2014) Event layers in the Japanese Lake Suigetsu "SG06" sediment core: description, interpretation and climatic implications. *Quat Sci Rev* 83:157–170
- Scholz D, Hoffmann DL (2011) StalAge - an algorithm designed for construction of speleothem age models. *Quat Geochronol* 6:369–382
- Schrag DP, Adkins JF, McIntyre K, Alexander JL, Hodell DA, Charles CD, McManus JF (2002) The oxygen isotopic composition of seawater during the Last Glacial Maximum. *Quat Sci Rev* 21:331–342
- Seierstad IK, Abbott PM, Bigler M, Blunier T, Bourne AJ, Brook E, Buchardt SL, Buizert C, Clausen HB, Cook E, Dahl-Jensen D, Davies SM, Guillevic M, Johnsen SJ, Pedersen DS, Popp TJ, Rasmussen SO, Severinghaus JP, Svensson A, Vinther BM (2014) Consistently dated records from the Greenland GRIP, GISP2 and NGRIP ice cores for the past 104 ka reveal regional millennial-scale $\delta^{18}\text{O}$ gradients with possible Heinrich event imprint. *Quat Sci Rev* 106:29–46
- Seki A, Tada R, Kurokawa S, Murayama M (2019) High-resolution Quaternary record of marine organic carbon content in the hemipelagic sediments of the Japan Sea from bromine counts measured by XRF core scanner. *Prog Earth Planet Sci* 6:1
- Shen CC, Edwards RL, Cheng H, Dorale JA, Thomas RB, Moran SB, Weinstein SE, Edmonds HN (2002) Uranium and thorium isotopic and concentration measurements by magnetic sector inductively coupled plasma mass spectrometry. *Chem Geol* 185:165–178
- Shen CC, Cheng H, Edwards RL, Moran SB, Edmonds HN, Hoff JA, Thomas RB (2003) Measurement of attogram quantities of ^{231}Pa in dissolved and particulate fractions of seawater by isotope dilution thermal ionization mass spectroscopy. *Anal Chem* 75:1075–1079
- Shen CC, Kano A, Hori M, Lin K, Chiu TC, Burr GS (2010) East Asian monsoon evolution and reconciliation of climate records from Japan and Greenland during the last deglaciation. *Quat Sci Rev* 29:3327–3335
- Shen CC, Wu CC, Cheng H, Edwards RL, Hsieh YT, Gallet S, Chang CC, Li TY, Lam DD, Kano A, Hori M, Spötl C (2012) High-precision and high-resolution carbonate ^{230}Th dating by MC-ICP-MS with SEM protocols. *Geochim Cosmochim Acta* 99:71–86
- Sone T, Kano A, Okumura T, Kashiwagi K, Hori M, Jiang X, Shen CC (2013) Holocene stalagmite oxygen isotopic record from the Japan Sea side of the Japanese Islands, as a new proxy of the East Asian winter monsoon. *Quat Sci Rev* 75:150–160
- Sone T, Kano A, Kashiwagi K, Mori T, Okumura T, Shen CC, Hori M (2015) Two modes of climatic control in the Holocene stalagmite record from the Japan Sea side of the Japanese islands. *Isl Arc* 24:342–358
- Steinke S, Mohtadi M, Groenewald J, Lin LC, Löwemark L, Chen MT, Rendle-Bühning R (2010) Reconstructing the southern South China Sea upper water column structure since the Last Glacial Maximum: implications for the East Asian winter monsoon development. *Paleoceanography* 25:1–15
- Steinke S, Glatz C, Mohtadi M, Groenewald J, Li Q, Jian Z (2011) Past dynamics of the East Asian monsoon: no inverse behaviour between the summer and winter monsoon during the Holocene. *Glob Planet Change* 78:170–177
- Sun Y, Clemens SC, Morrill C, Lin X, Wang X, An Z (2012) Influence of Atlantic meridional overturning circulation on the East Asian winter monsoon. *Nat Geosci* 5:46–49
- Tada R, Koizumi I, Cramp A, Rahman A (1992) Correlation of dark and light layers, and the origin of their cyclicity in the Quaternary sediments from the Japan Sea. *Proc ODP Sci Results* 127/128(1):577–601
- Tada R, Irino T, Koizumi I (1999) Land-ocean linkages over orbital and millennial timescales recorded in late Quaternary sediments of the Japan Sea. *Paleoceanography* 14:236–247
- Tada R, Zheng H, Clift PD (2016) Evolution and variability of the Asian monsoon and its potential linkage with uplift of the Himalaya and Tibetan Plateau. *Prog Earth Planet Sci* 3:4
- Tada R, Irino T, Ikehara K, Karasuda A, Sugisaki S, Xuan C, Sagawa T, Itaki T, Kubota Y, Lu S, Seki A, Murray RW, Alvarez-Zarikian C, Anderson WT Jr, Bassetti M-A, Brace BJ, Clemens SC, da Costa Gurgel MH, Dickens GR, Dunlea AG, Gallagher SJ, Giosan L, Henderson ACG, Holbourn AE, Kinsley CW, Lee GS, Lee KE, Lofi J, Lopes CID, Pellitero MS, Peterson LC, Singh RK, Toucanne S, Wan S, Zheng H, Ziegler M (2018) High-resolution and high-precision correlation of dark and light layers in the Quaternary hemipelagic sediments of the Japan Sea recovered during IODP Expedition 346. *Prog Earth Planet Sci* 5:19
- Tian J, Huang E, Pak DK (2010) East Asian winter monsoon variability over the last glacial cycle: Insights from a latitudinal sea-surface temperature gradient across the South China Sea. *Paleogeogr Palaeoclimatol Palaeoecol* 292:319–324
- Wang YJ, Cheng H, Edwards RL, An ZS, Wu JY, Shen CC, Dorale JA (2001) A high-resolution absolute-dated Late Pleistocene monsoon record from Hulu Cave, China. *Science* 294:2345–2348
- Wang Y, Cheng H, Edwards RL, Kong X, Shao X, Chen S, Wu J, Jiang X, Wang X, An Z (2008) Millennial- and orbital-scale changes in the East Asian monsoon over the past 224,000 years. *Nature* 451:1090–1093
- Xing L, Zhang R, Liu Y, Zhao X, Liu S, Shi X, Zhao M (2011) Biomarker records of phytoplankton productivity and community structure changes in the Japan Sea over the last 166 kyr. *Quat Sci Rev* 30:2666–2675

- Yamamoto M, Sai H, Chen MT, Zhao M (2013) The east Asian winter monsoon variability in response to precession during the past 150 000 yr. *Clim Past* 9: 2777–2788
- Yancheva G, Nowaczyk NR, Mingram J, Dulski P, Schettler G, Negendank JFW, Liu J, Sigman DM, Peterson LC, Haug GH (2007) Influence of the intertropical convergence zone on the East Asian monsoon. *Nature* 445:74–77
- Zhao S, Liu Z, Colin C, Zhao Y, Wang X, Jian Z (2018) Responses of the East Asian summer monsoon in the low-latitude south china sea to high-latitude millennial-scale climatic changes during the last glaciation: evidence from a high-resolution clay mineralogical record. *Paleoceanogr Paleoclimatology* 33:745–765

Publisher's Note

Springer Nature remains neutral with regard to jurisdictional claims in published maps and institutional affiliations.

Submit your manuscript to a SpringerOpen[®] journal and benefit from:

- Convenient online submission
- Rigorous peer review
- Open access: articles freely available online
- High visibility within the field
- Retaining the copyright to your article

Submit your next manuscript at ► [springeropen.com](https://www.springeropen.com)